GL-TR-89-0120

APPLICATION OF OPTICAL MEASURE THEORY TO ATMOSPHERIC TEMPERATURE SOUNDING FROM TOVS RADIANCES

Robert G. Hohlfeld
Thomas W. Drueding
John F. Ebersole

Creative Optics, Inc.
32 Wildwood Drive
Bedford, MA 01730

Final Report
December 1988-May 1989

2 May 1989

GEOPHYSICS LABORATORY
AIR FORCE SYSTEMS COMMAND
UNITED STATES AIR FORCE
HANSCOM AFB, MASSACHUSETTS 01731-5000

"This technical report has been reviewed and is approved for publication"

JEAN I.F. KING
Contract Manager

FOR THE COMMANDER

DONALD A. CHISHOLM, Acting Director
Atmospheric Sciences Division

This report has been reviewed by the ESD Public Affairs Office (PA) and is releasable to the National Technical Information Service (NTIS).

Qualified requestors may obtain additional copies from the Defense Technical Information Center. All others should apply to the National Technical Information Service.

If your address has changed, or if you wish to be removed from the mailing list, or if the addressee is no longer employed by your organization, please notify AFGL/DAA, Hanscom AFB, MA 01731. This will assist us in maintaining a current mailing list.

Do not return copies of this report unless contractual obligations or notices on a specific document requires that it be returned.

UNCLASSIFIED

SECURITY CLASSIFICATION OF THIS PAGE

REPORT DOCUMENTATION PAGE

1a. REPORT SECURITY CLASSIFICATION UNCLASSIFIED	1b. RESTRICTIVE MARKINGS
2a. SECURITY CLASSIFICATION AUTHORITY N/A	3. DISTRIBUTION/AVAILABILITY OF REPORT Approved for public release; distribution unlimited.
2b. DECLASSIFICATION/DOWNGRADING SCHEDULE N/A	
4. PERFORMING ORGANIZATION REPORT NUMBER(S) COI-SR-31	5. MONITORING ORGANIZATION REPORT NUMBER(S) GL-TR-89- 0120
6a. NAME OF PERFORMING ORGANIZATION Creative Optics, Inc. — 6b. OFFICE SYMBOL (If applicable)	7a. NAME OF MONITORING ORGANIZATION Geophysics Laboratory
6c. ADDRESS (City, State and ZIP Code) 32 Wildwood Drive Bedford, MA 01730	7b. ADDRESS (City, State and ZIP Code) Hanscom AFB Massachusetts 01731-5000
8a. NAME OF FUNDING/SPONSORING ORGANIZATION Geophysics Laboratory — 8b. OFFICE SYMBOL (If applicable) LY	9. PROCUREMENT INSTRUMENT IDENTIFICATION NUMBER F19628-88-C-0151
8c. ADDRESS (City, State and ZIP Code) Hanscom Air Force Base, MA 01731 -5000	10. SOURCE OF FUNDING NOS. PROGRAM ELEMENT NO.: 65502F — PROJECT NO.: 5502 — TASK NO.: 05 — WORK UNIT NO.: BB
11. TITLE (Include Security Classification) "Application of Optical Measure Theory to Atmospheric Temperature (cont. on reverse)	
12. PERSONAL AUTHOR(S) Robert G. Hohlfeld, Thomas W. Drueding, John F. Ebersole	
13a. TYPE OF REPORT Final — 13b. TIME COVERED FROM DEC 88 TO MAY 89 — 14. DATE OF REPORT (Yr., Mo., Day) 1989 MAY 2 — 15. PAGE COUNT 34	
16. SUPPLEMENTARY NOTATION	
17. COSATI CODES FIELD / GROUP / SUB GR.	18. SUBJECT TERMS (Continue on reverse if necessary and identify by block number) Minimization, Optical Measure Theory, Remote Sensing, Atmospheric Temperature Profiles.

19. ABSTRACT (Continue on reverse if necessary and identify by block number)

We have demonstrated robust algorithms for generating fits in Optical Measure Theory (OMT) to radiance data from the TIROS Operational Vertical Sounder (TOVS). These algorithms generated physically meaningful fits on 100% of a test set of 45 TOVS radiance scans, and were successful both on short wavelength (667/cm^{-1}) and on long wavelength (2250/cm^{-1}) TOVS data. The resulting OMT temperature profiles exhibit meteorological characteristics and appear to be suitable for determination of atmospheric structure parameters characterizing the large-scale vertical temperature structure of the atmosphere, and also suitable for generation of input data for numerical weather prediction codes.

Keywords: Optical data; [illegible] Meteorological satellites;

20. DISTRIBUTION/AVAILABILITY OF ABSTRACT UNCLASSIFIED/UNLIMITED ☐ SAME AS RPT. ☒ DTIC USERS ☐	21. ABSTRACT SECURITY CLASSIFICATION UNCLASSIFIED
22a. NAME OF RESPONSIBLE INDIVIDUAL Dr. Jean I. F. King	22b. TELEPHONE NUMBER (Include Area Code) 617/377-2976 — 22c. OFFICE SYMBOL GL/LY

DD FORM 1473, 83 APR — EDITION OF 1 JAN 73 IS OBSOLETE. — UNCLASSIFIED

SECURITY CLASSIFICATION OF THIS PAGE

11. Title (cont.)
Sounding from TOVS Radiances"

ACKNOWLEDGMENTS

We wish to acknowledge technical discussions with Dr. Jean I.F. King of the U.S. Air Force Geophysics Laboratory Atmospheric Sciences Division who was the Contracting Officer's Technical Representative. Mr. Vincent Falcone, also of the AFGL Atmospheric Sciences Division, and alternate COTR, contributed important scientific commentary.

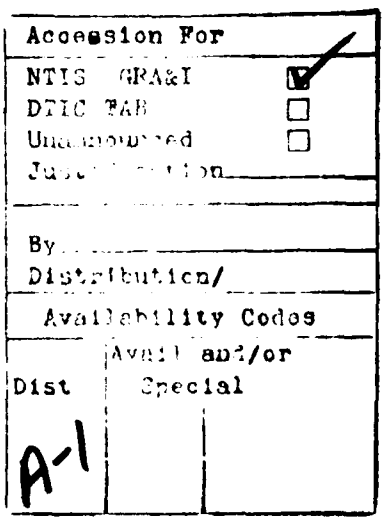

TABLE OF CONTENTS

EXECUTIVE SUMMARY

We have demonstrated robust algorithms for generating fits in Optical Measure Theory (OMT) to radiance data from the TIROS Operational Vertical Sounder (TOVS). These algorithms generated physically meaningful fits on 100% of a test set of 45 TOVS radiance scans, and were successful both on short wavelength (700 cm^{-1}) and on long wavelength (2250 cm^{-1}) TOVS data. The resulting OMT temperature profiles exhibit meteorological characteristics and appear to be suitable for determination of atmospheric structure parameters characterizing the large-scale vertical temperature structure of the atmosphere, and also suitable for generation of input data for numerical weather prediction codes.

1. INTRODUCTION

The mathematical difficulties encountered in attempting to invert satellite radiance data to obtain atmospheric temperature profiles have been of considerable theoretical interest to the mathematical and satellite meteorology communities. In this report we outline the application of a new approach to the solution of this problem, Optical Measure Theory (OMT), which has been invented by Dr. J. I. F. King of the Air Force Geophysics Laboratory (King 1989 ; Leon and King 1988).

The upwelling radiance is determined by the equation of radiative transfer, which is a Fredholm integral equation of the first kind, integrating over the Planck function as a function of height. The mathematical difficulties in carrying out inversions stem from this simple physical description. Since integration is intrinsically a smoothing operation, the radiance profile will tend to be smoother, qualitatively speaking, than the atmospheric temperature profile which generates it. Furthermore, since the solutions of these integral equations are not unique, many atmospheric temperature profiles (in fact, formally an uncountably infinite set) can give rise to the same radiance profile, and thus cannot be distinguished on the basis of radiance observations.

Clearly, a radiance profile has only a limited information content, relative to the problem of reconstructing the atmospheric temperature profile. (We intend to make this statement mathematically rigorous in later research by an information theoretical analysis, which will address the actual information content, in bits, of radiance observations.) Therefore, construction of an atmospheric temperature profile which replicates the detailed structure of an *in situ* radiosonde observation is probably unrealistic, however, extracting information about the overall morphology of the atmospheric temperature profile is a meaningful objective within the context of present theoretical developments. We expect that this overall morphological information concerning the atmospheric temperature profile may be expressed in terms of "atmospheric structure parameters", such as temperature lapse rates and tropopause temperatures and pressures, which are meaningful quantities in meteorological research. Furthermore, these quantities are appropriate input parameters for numerical weather prediction codes, which are in any event insensitive to the small-scale atmospheric temperature structures which are found in radiosonde temperature profiles.

OMT has a number of desirable theoretical features that make it especially appropriate as an approach to the inversion problem. In OMT, a smooth functional form is fit to the radiance profile; thus, OMT represents one approach for solution of the inversion problem by regularization, in the sense that the space of possible solutions is restricted by the imposition of reasonable physical constraints. This restriction of the class of functions used in representing the radiance profiles is also reflected in a restriction of the class of functions used in the representation of the atmospheric temperature profiles. In effect, we select the smoothest possible representation of the radiance profile consistent with the radiance data set at an appropriate level of confidence. Crudely speaking, this represents a "least information" representation in the sense that we have imposed a minimum of information not actually present in the radiance measurements in the process of carrying out our smoothing through a functional fit to the radiance data. The resulting atmospheric temperature is then also "bias-free" in the sense that it contains no *a priori* information concerning the temperature structure of the atmosphere. Such a representation may fairly be said to have been constructed if the functions from which the radiance representation is constructed, which we term "basis functions", are chosen on grounds of fundamental physical principles describing the problem. In fact, in OMT this choice is made on the basis of the mathematical description of a radiative atmosphere.

It is important to note that in OMT we have imposed the constraints of functional smoothness on the radiance data, that is, as close to the instrument as possible. All remaining transformations in OMT required for the calculation of atmospheric temperature profiles are strictly one-to-one transformations (and hence information-conserving). OMT is theoretically advantageous in this regard also because the relation between the theoretical results of OMT and instrumental characteristics is particularly clear and straightforward in principle.

The functional representation for the atmospheric temperature profiles is calculated from the radiance profile basis functions by a generalization of the Laplace transform. This transformation is motivated by realizing that for a large class of atmospheric weight functions, the equation of radiative transfer may be viewed as an integral transform, specifically a generalization of the Laplace transform. This observation is one of the crucial theoretical insights contained in OMT. As a result, the choice of basis functions used in the representation of the radiance profile and in the representation of the atmospheric temperature profile may not be made independently; the temperature profile basis functions are (generalized) inverse Laplace transforms of the radiance profile basis functions. In this sense, OMT may be said to be an algebra of radiance profiles, since profile-like functional forms are fundamental entities of OMT.

We shall demonstrate in this report how OMT may be used to construct atmospheric temperature profiles which have an overall morphology characteristic of observed atmospheric temperature profiles and which may be sued to obtain atmospheric structure parameters suitable for input to numerical weather prediction codes. In the study reported on here, the radiance data analyzed were obtained from the TIROS Operational Vertical Sounder (TOVS), however, the general principles may be applied to other atmospheric sounders, such as on the DMSP satellites. We have demonstrated robust algorithms which yield valid OMT solutions from TOVS radiance data with reasonably high probability. Additional research will improve the computational efficiency and robustness of OMT and generate further applications in satellite meteorology and numerical weather prediction.

2. THEORY

2.1 Introduction and Development of Optical Measure Theory. In this subsection, we include for completeness a derivation of Dr. King's OMT (King 1989; King and Leon 1988). In OMT we attempt to invert the equation of radiative transfer

$$R(P) = \int_0^\infty W(p/P)B(p) \frac{dp}{p} \tag{1}$$

where R is the observed radiance and B the Planck function. It is convenient to parametrize this problem in terms of the atmospheric pressure, p, rather than altitude. Equation (1) represents the radiance observed in a single channel of a radiometer measuring the upwelling radiance at the top of the atmosphere. W is a weight function for that channel and P is a characteristic pressure value for that channel, crudely speaking the centroid of the weight function. (Our work contains significant new developments in the definition of P, discussed in Section 2.3.) The weight function is defined to be

$$W = - \frac{\partial \tau}{\partial \ln p} \tag{2}$$

where τ is the atmospheric transmittance. Thus W measures the interaction between the radiation field and atmospheric material.

It is often convenient to parametrize the weight function in terms of a generalized exponential weight function

$$W_m(p/P) = W_m(x) = \frac{m^m}{\Gamma(m+1)} x \exp(-mx^{1/m}) \tag{3}$$

where $x = p/P$ and m is a fitting parameter controlling the width of the generalized exponential weight function, and Γ denotes the usual Γ function (King 1985; King, Hohlfeld, and Kilian 1989). This simple functional form captures the essential physical character of atmospheric weight functions in many cases. (For $m = 1$ this formula reduces to a simple exponential weighting function.) While OMT bay be carried out with completely general weight functions, for the generalized exponential weight functions of the form given in equation (3) the derivation is particularly clear.

When we substitute the generalized exponential weight function into the equation of radiative transfer, we obtain

$$R(P) = \frac{m^m}{\Gamma(m+1)\, P} \int_0^\infty B(p) \exp[-m(p/P)^{1/m}] \tag{4}$$

For $m = 1$, Eq. (4) immediately assumes the character of a Laplace transform,

$$R(P) = \frac{1}{P}\int_0^\infty B(p)e^{-(p/P)}\,dp \tag{5}$$

i.e. $PR(P)$ is the Laplace transform of $B(p)$ with respect to the transform variable $1/P$. When $m \neq 1$, the radiance profile and Planck function profile are then related by a generalization of the Laplace transform defined in terms of the generalized exponential function. All of the useful analytic properties of the Laplace transform are retained in this generalization of the Laplace transform utilizing the generalized exponential function kernel.

If a choice of functional form is made for $B(p)$ (or alternatively $R(P)$), equation (4) then immediately implies the functional form $R(P)$ (alternatively $B(p)$) must assume. This observation is especially pertinent if we note that the Planck function profile of a radiative atmosphere is exponential in form, *i.e.*

$$B(p) = Le^{-kp} \tag{6}$$

with k and L constants (Chandrasekhar 1960). The corresponding ($m = 1$) radiance profile function is then,

$$R(P) = \frac{L}{1+kP} \tag{7}$$

This discussion motivates a choice of the functional form by which radiance data is represented (King 1989; King and Leon 1988),

$$R(P) = a + bP + \sum_{i=1}^{j} \frac{L_i}{1+k_iP} \tag{8}$$

where j hyperbolic terms are included. The addition of a linear term of form $a + bP$ (with a and b constants) was found by King and Leon to be of practical utility in the representation of radiance data. Generalization to the inclusion of a polynomial of arbitrary order in P is straightforward. The corresponding Planck function profile obtained by generalized inverse Laplace transformation (for arbitrary m) of Eq. (7) is

$$B(p) = a + bp + \sum_{i=1}^{j} L_iE_m(-k_ip) \tag{9}$$

Where $E_m(x)$ is the generalized exponential function with parameter m. This new function is discussed and its general properties exhibited in the following section.

The choice of an exponential (or generalized exponential form of the Planck function profile, motivated by the expectation of the real atmospheric acting at least in part as a radiative atmosphere, indicates that Eq. (8) is a natural choice of functional form for the representation of radiance data.

2.2 The Generalized Exponential Function and the Calculation of Atmospheric Temperature Profiles. In this section we briefly describe some of the properties of the generalized exponential function introduced in the previous section. The generalized exponential weighting function, $E_m(x)$, has a power series expansion

$$E_m(x) = \frac{1}{\Omega_m(1)} + \frac{x}{\Omega_m(2)} + \frac{x^2}{\Omega_m(3)} + \cdots + \frac{x^n}{\Omega_m(n+1)} + \cdots \tag{10}$$

where the Ω_m's are defined in terms of moments of the generalized exponential weight functions by

$$\Omega_m(n+1) = \int_0^\infty x^n \, W_m(x) \, \frac{dx}{x} . \tag{11}$$

It is apparent that equation (10) represents a generalization of the usual exponential function, e^x, if we write the series expansion of e^x using $\Gamma(n+1)$ to represent $n!$,

$$e^x = \frac{1}{\Gamma(1)} + \frac{x}{\Gamma(2)} + \frac{x^2}{\Gamma(3)} + \cdots + \frac{x^n}{\Gamma(n+1)} + \cdots \tag{12}$$

and note that $\Gamma(n)$ is defined by its integral representation

$$\Gamma(n) = \int_0^\infty t^{n-1} \, e^{-t} \, dt , \tag{13}$$

and so $E_1(x) = e^x$. This motivates the form of equation (9). We plot in Figure 1 a family of curves of $E_m(x)$ for various values of m. It is apparent from this plot that variation of m controls the stiffness of the resulting Planck function curve.

The definition of the generalized exponential function discussed here is motivated by the functional form of the generalized weight function $W_m(x)$. However, an empirically obtained weight function of general form may also be reduced to a collection of moments and a corresponding function $E(x)$ computed, and so this development of OMT is not restricted simply to the use of generalized exponential weight functions.

Once a fit has been made to the radiance data on the basis of the form of equation (8), translation into the form of the Planck function profile given by equation (9) is immediate, provided that we have determined m values for the evaluation of $E_m(-kp)$ based on a fit to the atmospheric weight functions characterizing the instrumental channels used in the fit. A wavenumber is then chosen (usually the wavenumber of the central channel, to which radiance measurements are normalized) and the Planck formula,

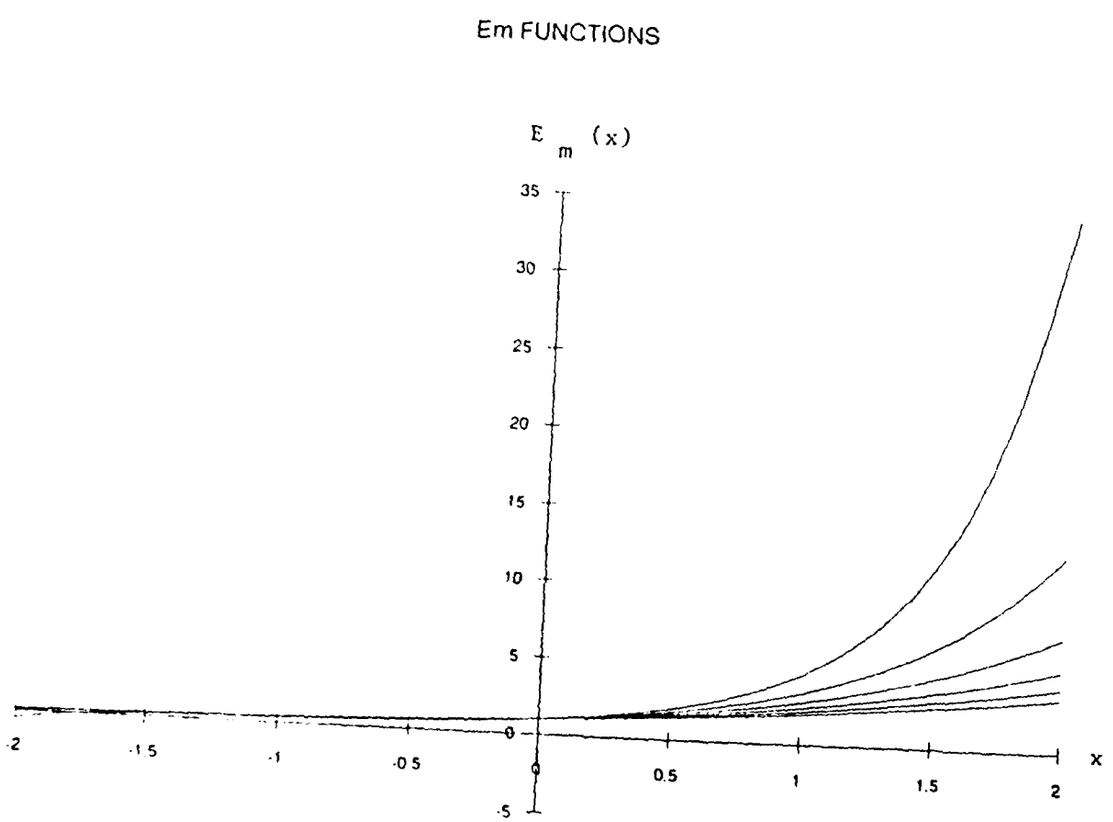

Figure 1: Family of plots of the generalized exponential function $E_m(x)$ of OMT. Curves are shown for values of m = 0.5, 0.75, 1.0, 1.25, 1.5, and 1.75. Small values of m correspond to the largest values of $E_m(x)$, at large x. It may be seen that variation of m yields members of an exponential family of curves with varying degrees of "stiffness".

$$B = \frac{c_1 \nu^3}{\exp\left(\frac{c_2 \nu}{T}\right) - 1} , \qquad (14)$$

for a given height (parametrized by its pressure p), may be solved for the temperature at that height. Here ν is the wavenumber, and c_1 and c_2 are constants with values, $c_1 = 1.19107 \times 10^{-5}$ erg·cm^2/sec·sr and $c_2 = 1.438858$ cm·K, and T in degrees Kelvin. The mathematical formalism outlined here gives a clear path from the radiance measurements to the specification of the temperature as a function of height in the atmosphere. It is important to note that the OMT transformation [of equation (8) to equation (9)] and the solution of the atmospheric temperature profile from the Planck function profile are one-to-one transformations, *i.e.* given a particular choice of radiance basis functions, as in equation (8), once a fit is made to that functional form, the atmospheric temperature profile, $T = T(h)$, is uniquely determined.

2.3 Definition of *P* Values. In work undertaken on Differential Inversion and OMT to date (King, Hohlfeld, and Kilian 1989) P has been defined as that value of the pressure at which the weight function achieves its maximum value. We have noted that this definition is not entirely satisfactory in that some weight functions may have a complicated geometric form, and may in fact exhibit multiple maxima, particularly if several absorbing chemical species are present.

In view of the character of equation (1), the equation of radiative transfer, which specifies the generation of the upwelling radiance based on the distribution of temperature versus height in the atmosphere, we have begun investigations of more suitable definitions of P based on moments of the weight function. In particular, if we consider equation (1) for the case of an isothermal atmosphere, $B(p)$ will be a constant function, and the contributions to $R(P)$ will be centered about the center of mass of the weight function, *i.e.* the centroid. This suggests that the centroid of the weight function ought to be chosen as a value for P, and this definition is attractive in that it is well defined even for weight functions which have complicated geometries with multiple maxima. Given the definition of the weight function, as in equation (2), it is apparent that this definition is equivalent to selection of that pressure value at which $\tau = 1/2$.

At present, this argument is suggestive, rather than rigorous. However, we have noted in our research efforts attempting to construct OMT fits to TOVS radiance data, that superior fits, in the sense of having lower χ^2 values, were obtained using these P values defined in terms of the centroid of the TOVS weight functions. Further research will be required during the Phase II effort to investigate rigorously appropriate definitions of P. This problem is of special significance for weight functions which have significant values at ground level (and are therefore truncated at ground level with significant loss of the area under the weight function curve).

2.4 Development of the Nonlinear Least Squares Nonlinear Hyperbolic Algorithm (NLLS NHA)

2.4.1 Motivation. Leon and King (1988) have investigated an algorithm for directly fitting a formula of the form of equation (8) to radiance data, and despite the attractive adaptive features of that algorithm, the requirements on the accuracy of the radiance values are severe. This property arises from the character of the Leon and King Nonlinear Hyperbolic Algorithm (NHA) as an interpolation formula; the solution resulting from the NHA is constrained to pass

identically through each of the radiance values. In practice, radiance data are corrupted by noise (usually with Gaussian statistics) and the requirement of passing through each data point is unnecessarily stringent under some circumstances.

Furthermore, fitting a formula of the form of equation (8) is a difficult numerical problem. Fitting a sum of exponential functions to a collection of data is a classical example of an ill-conditioned fitting problem (Acton 1970). This problem is very similar because e^{-x} and $1/(1 + x)$ have very similar shapes over the first octave of their range. Consequently, this problem may be expected to exhibit similar ill-conditionedness, as is in fact observed.

Motivated by these considerations, we have begun development of a new algorithm for fitting radiance data to a formula of the form of equation (1) based on nonlinear least squares techniques (Hohlfeld, Kilian, Drueding, and Ebersole 1988). We have named this algorithm the NLLS NHA. The intent of the NLLS NHA is to fit as many terms of the formula of equation (1) as can be supported by the radiance data set, as determined by objective criteria of the "goodness of fit", such as measures of χ^2. Ultimately, based on the development of NLLS NHA techniques, it will be possible to derive measures of the information content of a radiance data set based on the number of well conditioned terms of the fit which can be obtained.

Nonlinear least squares fitting algorithms operate by the minimization of an appropriately constructed cost function, usually termed χ^2, defined by

$$\chi^2 = \sum_{i=1}^{n} \left[\frac{y_i - y(a_1,\ldots a_k,x_i)}{\sigma_i} \right]^2 \qquad (14)$$

The algorithm seeks to minimize χ^2, by varying the k parameters of the theory, $a_1,\ldots,a_k$, and a total of n measurements have been taken at n values of independent variable, x_i, to obtain values of the dependent variable, y_i. The description of the model is contained in the function $y(a_1,\ldots a_k,x)$.

Choice of the appropriate algorithm for achieving χ^2 minimization in a given functional fitting problem is most readily made on the basis of an investigation of the geometric properties of the χ^2 surface. The information required for making such a choice of algorithm is described below.

2.4.2. Selection of the Levenberg-Marquardt Algorithm for the NLLS NHA. Work undertaken earlier in this project has characterized the geometry of the χ^2 surface generated by attempting to fit a functional form of the radiance data, as given by equation (8) to radiance data from the TIROS Operational Vertical Sounder (TOVS). We have found that the characteristic size of the minima in a and the L's for the positive k portion of the radiance χ^2 surface is typically of the order of a few tens in magnitude and the minima in the k's are of the order of unity in characteristic width. Minima in the radiance χ^2 surface with $k < 0$ (see section 3.1) are much more constrained in L (width < 10) and in k (width < 1/2). Multiple deep minima in χ^2 exist in close proximity in this region. (See Figure 2.) The geometry of the χ^2 surfaces in the immediate neighborhood of the minima is regular and the ellipses defined by levels of constant χ^2 are reasonably well aligned from one level to the next.

In Figure 3 we show the χ^2 surface generated by comparing the temperature profile corresponding to the radiances generating Figure 2 against the corresponding radiosonde observations. It is important to note that the minimum in the temperature χ^2 surface coincides with the global minimum in the radiance χ^2 surface shown in Figure 2, thus confirming our identification of the correct physical solution in the OMT processing of this radiance scan.

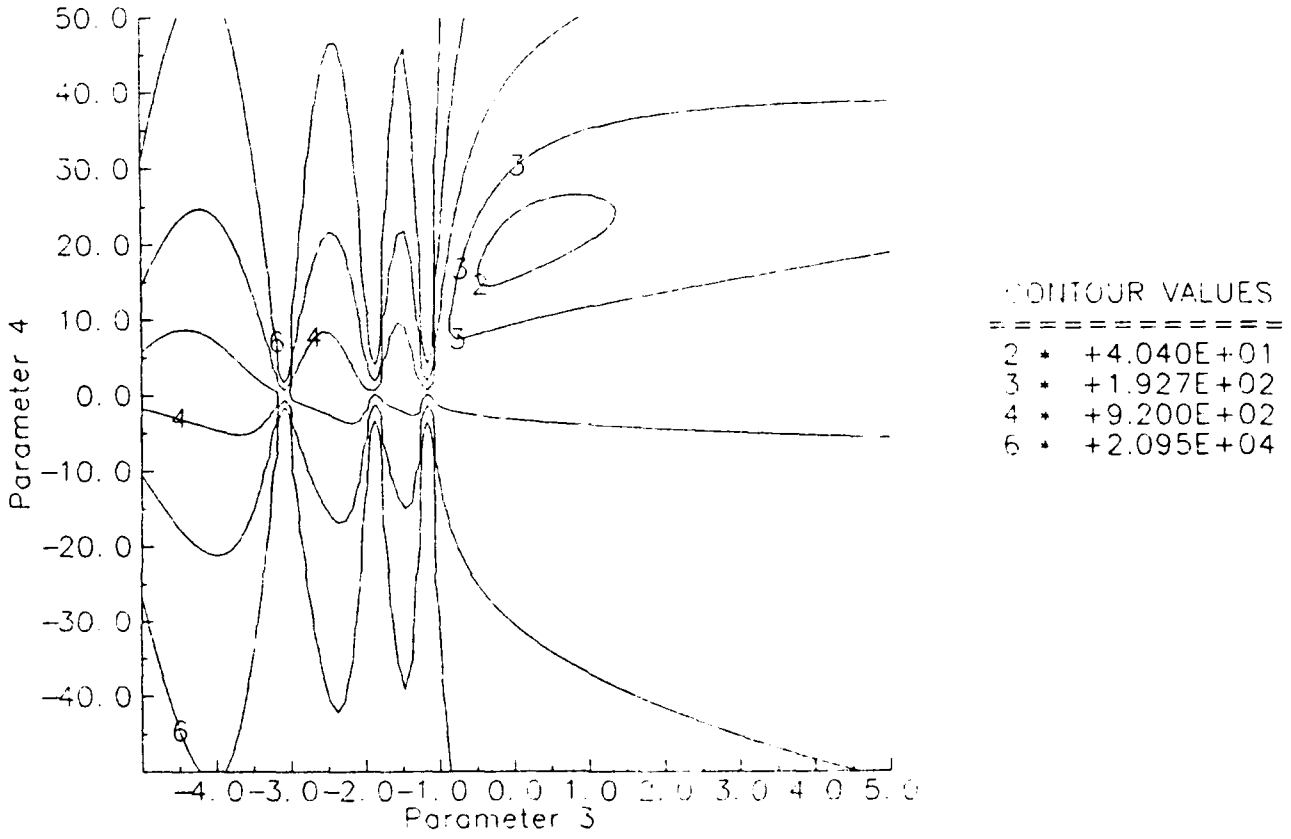

Figure 2: χ^2 surface of the Optical Measure Theory fit to a radiance profile. Shown here is a contour map of the χ^2 surface generated using OMT with four parameters to fit a radiance profile. The TOVS radiance scan from Zone 1 Pass 9 was chosen for this example. Two parameters are held constant (a = 20 and b = 45) and two are varied (K_1 ranging from -5 to 5 and L_1 ranging from -50 to 50). The geometry seen here is representative of all the TOVS scans.

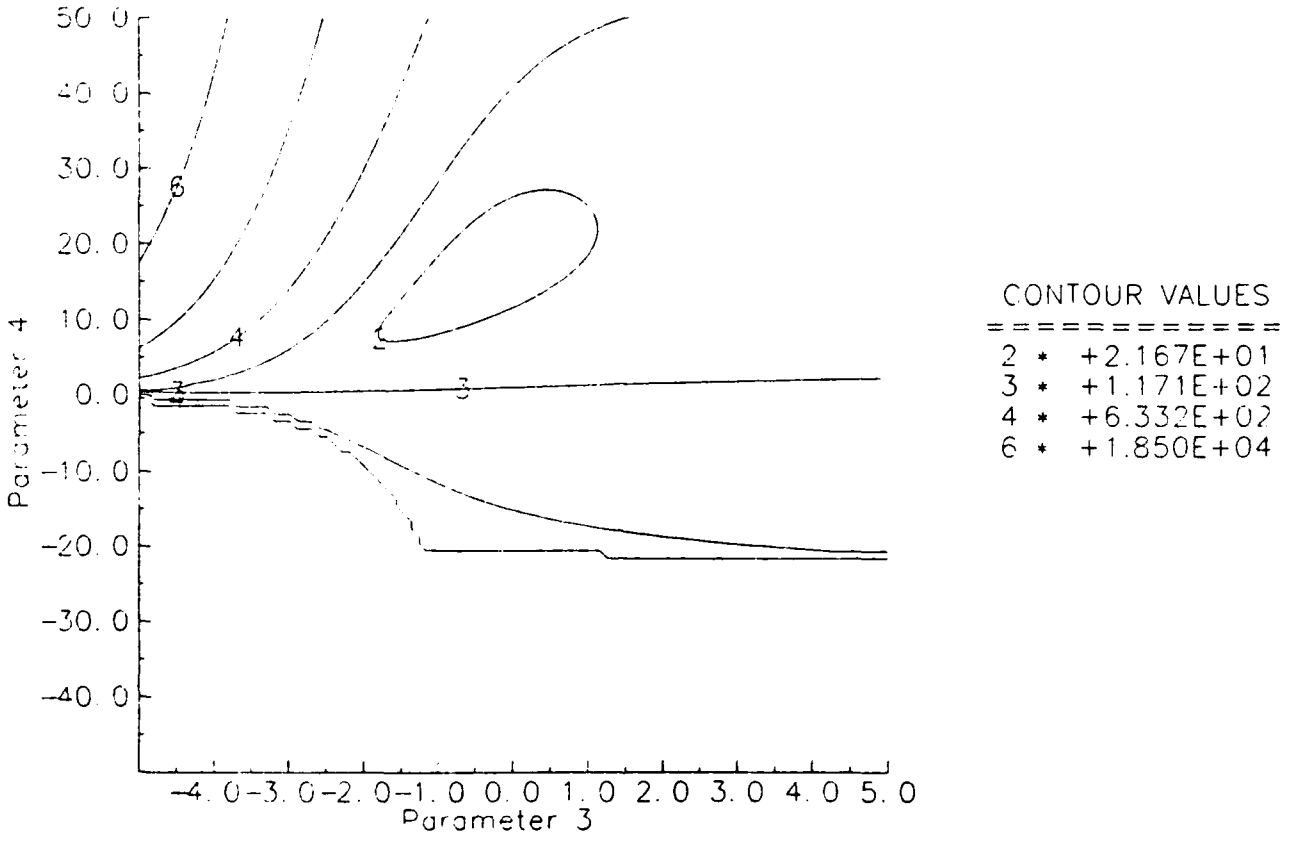

Figure 3: χ^2 surface of the Optical Measure Theory fit to the temperature profile from RAOB data. Shown here is the contour map of the χ^2 surface generated using OMT to fit a temperature profile from RAOB data under the same conditions as Figure 2.

Owing to this comparatively well-behaved geometry in the χ^2 surfaces, we are motivated to select a comparatively conventional but well-tested algorithm for the χ^2 minimization in the NLLS NHA, the Levenberg-Marquardt algorithm. This algorithm is discussed by Press, Flannery, Teukolsky, and Vetterling (1986), and we reproduce some relevant elements of their discussion in the following section to motivate our choice of this algorithm for the NLLS NHA.

2.4.3 Development of the Levenberg-Marquardt Algorithm. We consider here the general case when a model depends *nonlinearly* on a set of M unknown parameters a_k, $k = 1,2,...,M$. [The parameters a_k correspond to the parameters a, b, k_1, L_1, k_2 and L_2 in equation (9).] Our objective is to minimize the χ^2 merit function, as defined in equation (14), and thereby to determine the best-fit parameters for the fit of our model. Since the model is nonlinear, it is necessary to carry out an iterative solution for our desired parameters. Given trial values for the parameters, some procedure improving the trial solution is carried out until χ^2 stops (or effectively stops) decreasing.

Sufficiently close to the minimum, we can expect that the χ^2 function will be approximated by a quadratic form, which may be written as

$$\chi^2(\mathbf{a}) \simeq \gamma - \mathbf{d}\cdot\mathbf{a} + \frac{1}{2}\,\mathbf{a}\cdot\mathbf{D}\cdot\mathbf{a} \tag{16}$$

where $\mathbf{d}$ is an M-vector and $\mathbf{D}$ is an $M \times M$ matrix. If the approximation is a good one, we can jump from the current trial parameters $\mathbf{a}_{cur}$ to the minimizing ones $\mathbf{a}_{min}$ in a single step,

$$\mathbf{a}_{min} = \mathbf{a}_{cur} + \mathbf{D}^{-1}\cdot\left[-\nabla\chi^2(\mathbf{a}_{cur})\right] \tag{17}$$

On the other hand, equation (17) might be a poor local minimization to the shape of the function we are attempting to minimize at $\mathbf{a}_{cur}$. In such an instance, all that can be done is to take a step along the gradient of χ^2, as is done in the steepest descent method for minimization. In that case the next iteration would be given by

$$\mathbf{a}_{next} = \mathbf{a}_{cur} - \text{constant} \times \nabla\chi^2(\mathbf{a}_{cur}) \tag{18}$$

where the constant is chosen small enough so as to not exhaust the downhill direction.

To use either equation (17) or (18), we must be able to compute the gradient of the χ^2 function at any set of parameters $\mathbf{a}$. To use equation (4), we also need the matrix $\mathbf{D}$, the second derivative matrix (Hessian matrix) of the χ^2 merit function, at any $\mathbf{a}$. In the Levenberg-Marquardt method, we shall use either the Hessian matrix or the method of steepest descents for the minimization of χ^2, depending upon the information that can be extracted by the algorithm concerning the local geometry of the χ^2 surface.

The model to be fitted is

$$y = y(x;\mathbf{a}) \tag{19}$$

and the v2 merit function is given by

$$\chi^2(\mathbf{a}) = \sum_{i=1}^{N} \left[\frac{y_i - y(x_i;\mathbf{a})}{\sigma_i} \right]^2 \tag{20}$$

The gradient of χ^2 with respect to the parameters **a**, which will be zero at the χ^2 minimum, has components

$$\frac{\partial \chi^2}{\partial a_k} = -2 \sum_{i=1}^{N} \frac{[y_i - y(x_i;\mathbf{a})]}{\sigma_i^2} \frac{\partial y(x_i;\mathbf{a})}{\partial a_k} \tag{21}$$

Taking an additional partial derivative yields

$$\frac{\partial^2 \chi^2}{\partial a_k \partial a_l} = 2 \sum_{i=1}^{N} \frac{1}{\sigma_i^2} \left[\frac{\partial y(x_i;\mathbf{a})}{\partial a_k} \frac{\partial y(x_i;\mathbf{a})}{\partial a_l} - [y_i - y(x_i;\mathbf{a})] \frac{\partial^2 y(x_i;\mathbf{a})}{\partial a_l \partial a_k} \right] \tag{22}$$

It is conventional to remove the factors of 2 by defining

$$\beta_k \equiv -\frac{1}{2} \frac{\partial \chi^2}{\partial a_k} \tag{23}$$

and

$$\alpha_{kl} \equiv \frac{1}{2} \frac{\partial^2 \chi^2}{\partial a_k \partial a_l} \tag{24}$$

making $[\alpha] = (1/2)\mathbf{D}$ in equation (17), in terms of which that equation can be rewritten as the set of linear equations

$$\sum_{l=1}^{M} \alpha_{kl} \, \delta a_l = \beta_k \tag{25}$$

This set of equations is solved for the increments δa_l, which are added to the current approximation to obtain the next approximation to the set of parameters. In the context of least-squares fitting, the matrix [α], which is equal to one-half times the Hessian matrix, is usually called the curvature matrix.

Equation (18), the steepest descent formula may be expressed

$$\delta a_l = \text{constant} \times \beta_l \tag{26}$$

Note that the components α_{kl} of the Hessian matrix depend both on the first derivatives and on the second derivatives of the basis functions with respect to their parameters. Many treatments proceed to ignore the second derivative, without justification, which we shall attempt to supply here. Second derivatives occur because the gradient [equation (21)] already has a dependence of $\partial y_i/\partial a_k$, and so the next derivative must simply contain terms involving $\partial^2 y_i/\partial a_j \partial a_k$. The second derivative term can be neglected when it is zero (as in linear regression), or small enough to be negligible when compared to the term involving the first derivative. It also has an additional possibility of being ignorably small in practice: The term multiplying the second derivative in equation (22) is $[y_i - y(x_i;\mathbf{a})]$. For a successful model, this term should be just the random measurement error of each point. This error can have either sign, and should in general be uncorrelated with the model. Therefore, the second derivative terms tend to cancel out when summed over i.

Inclusion of the second-derivative term can in fact be destabilizing if the model fits badly or is contaminated by outlier points that are unlikely to be offset by compensating points of opposite sign. From this point on we shall always use as the definition of α_{kl} the formula

$$\alpha_{kl} = \sum_{i=1}^{N} \frac{1}{\sigma_i^2} \left[\frac{\partial y(x_i;\mathbf{a})}{\partial a_k} \frac{\partial y(x_i;\mathbf{a})}{\partial a_l} \right] \tag{27}$$

It should be understood that minor (or even major) fiddling with [α] has no effect at all on which final set of parameters **a** is reached, but only affects the iterative route that is taken getting there. The condition at the χ^2 minimum, that $\beta_k = 0$ for all k, is independent of how [α] is defined.

2.4.4 The Levenberg-Marquardt Method. An elegant method has been put forward by Marquardt (1963) based on an earlier suggestion by Levenberg, which combines smoothly the inverse-Hessian and steepest descent methods for χ^2 minimization, as discussed in the previous section. The steepest descent method is used far from the χ^2 minimum, when the geometry of the χ^2 is not well modeled by a locally quadratic behavior. Then, as the minimum is approached, the Levenberg-Marquardt algorithm is switched continuously to χ^2 minimization by the inverse-Hessian method. The Levenberg-Marquardt method works well in practice, and has become a standard nonlinear least-squares algorithm (Press, Flannery, Teukolsky, and Vetterling 1986).

Application of the Levenberg-Marquardt method depends upon two observations regarding the steepest descent and inverse-Hessian methods. Consider the constant multiplier in equation (26); within the context of a standard steepest descent implementation, we have no information regarding the magnitude of the constant or about the scale over which it may be applied. No

information answering these questions is available in the calculation of the gradient of χ^2, which tells us only the value of the slope of the χ^2 surface, not the distance that the slope extends. Marquardt's first insight is that the components of the Hessian matrix, even if they are not usable in any precise fashion, give some information regarding the order-of-magnitude scale of the problem.

The quantity χ^2 is dimensionless, *i.e.* is a pure number. On the other hand, β_k has the dimensions of $1/a_k$, which may be a dimensional quantity (and in fact each component of β_k may have different dimensions). The constant of proportionality between β_k and δa_k must therefore have the dimensions of a_k^2. In the components of $[\alpha]$, the obvious quantity with these dimensions is $1/\alpha_{kk}$, the reciprocal of the diagonal element, which must be the scale of the constant for the application of steepest descent. In practice, it is necessary to divide the constant by some (nondimensional) fudge factor λ, with the possibility of setting $\lambda >> 1$ to cut down the step size. In other words, replace equation (26) with

$$\delta a_l = \frac{1}{\lambda \alpha_{ll}} \beta_l \tag{28}$$

It is necessary that α_{ll} be positive, but this is guaranteed by our definition of equation (27), which was one of the motivations for making that choice.

The second insight in Marquardt's development of this algorithm is that equations (28) and (28) can be combined if we define a new matrix γ by the following prescription

$$\gamma_{jj} \equiv \alpha_{jj} \ (1 + \lambda)$$

$$\gamma_{jk} \equiv \alpha_{jk} \qquad (j \neq k) \tag{29}$$

and then replace both equations (25) and (28) by

$$\sum_{l=1}^{M} \gamma_{kl} \delta a_l = \beta_k \tag{30}$$

When λ is very large, the matrix γ is forced into being diagonally dominant, so that equation (30) goes over to the form of equation (28). On the other hand, as λ approaches zero, equation (30) goes over to the form of equation (25). What has been accomplished by use of γ in the χ^2 Levenberg-Marquardt algorithm is to have the minimization algorithm convert smoothly from the steepest descent algorithm to the inverse-Hessian minimization algorithm as the minimum in the χ^2 surface is approached.

2.4.5 Limitations of the Levenberg-Marquardt Method. Our development of the NLLS NHA has reduced the process of obtaining OMT solutions to the process of minimization on an appropriately defined χ^2 surface, which we accomplish by the Levenberg-Marquardt method. However, while the Levenberg-Marquardt method is a relatively sophisticated minimization technique, it still takes account only of locally defined information on the χ^2 surface, and each step in parameter space is made so as to reduce the value of χ^2 of the solution. Accordingly, it is possible for the solution to become "trapped" in a local minimum in the χ^2 surface, and thus never attain the true global solution. We circumvent this problem in our present research by

selection of appropriate starting vectors, motivated by our analysis of the χ^2 surface, which permit us to avoid the local minima, while still not biassing the solution. This procedure works with reasonably high probability, but is still somewhat *ad hoc*, and a more theoretically satisfactory alternative should be sought.

Simulated annealing (Metropolis *et al.* 1953) and neural network techniques (Hopfield and Tank 1985) have been applied to minimization problems in radiative transfer (Jeffrey and Rosner 1986). These techniques have been shown to yield true global minima with effectively unit probability. While these techniques are computationally intensive, being implemented most effectively in parallel computer architectures, they are of great interest and have potentially significant applications in the inversion problem.

3. ANALYSIS

3.1 New OMT Solutions. Our previous OMT solutions (Hohlfeld, Kilian, Drueding, and Ebersole 1988) exhibited the character of being a reasonable fit at the tropopause and for the temperature profile in the stratosphere (in the sense of fitting global morphological features of the temperature profile, rather than accounting for all the details of the radiosonde observations). However, these initial OMT fits deviated significantly from radiosonde measurements of the atmospheric temperature in the troposphere, by an amount increasing as the pressure increases, up to some tens of Kelvins at ground level. All such fits contained a single hyperbolic term, with a positive value for k_1.

Subsequent analysis has shown that a negative value for k_1 yields significantly improved fits to both the radiance profile and temperature profile (as measured by the χ^2 calculation in the NLLS NHA), particularly over the domain of tropospheric pressures. A value of k_1 less than zero may initially seem troubling theoretically in that it corresponds to a pole in the OMT radiance formula

$$R(P) = a + bP + \sum_{i=1}^{j} \frac{L_i}{1 + k_i P} \tag{31}$$

at positive P (*i.e.* at positive pressure). Here P is the pressure of the maxima of the radiance channels, suitably normalized (to a pressure of 1 bar for this work, so that $0 < P \leq 1$ over the physical atmosphere). Values of k_i such that $-1 < k_i < 0$, correspond to poles in $R(\mu)$ occurring below ground level, *i.e.* in an unobservable region

With the viewpoint that equation (1) constitutes a rational function representation of the radiances over the observed pressure range, the existence of a pole in the radiance formula for a value of the pressure at which radiance measurements cannot be obtained is not a cause for concern.

We note that in the present formulation of OMT, some difficulties arise due to the truncation of weight functions at ground level ($P = 1$). This prompts the speculation (albeit a reasonable one) that the negative k_1 values obtained in our OMT solutions arise due to this truncation of the atmospheric weight functions. This motivates an extension of OMT, beyond its present formulation, which more realistically treats the radiative transfer problem at the base of the atmosphere. Further research, undertaken during the Phase II effort, should clarify these important practical and theoretical issues.

3.2 Description of NLLS NHA Software.

3.2.1 Introduction. We have designed a computerized algorithmic framework to test different implementations of χ^2 minimization algorithms. This framework provides several options when running a algorithm. We look for a set of options which produce a good fit to the radiance data and are applicable to all available cases. The algorithms for the Non-Linear Least Squares, the Non-Linear Hyperbolic fitting, and a χ^2 analysis of a fit to radiance data are written in FORTRAN. We created a shell program to drive these routines, to report the results, and to quickly change the methods of implementation. The program runs in two modes, a highly interactive mode where we chose one scan and make immediate adjustments to our method and

a batch mode which analyzes all scans using one method. The batch mode also provides the means of processing the data when we determine an optimal robust reduction procedure using these algorithms. A spread sheet program (using Microsoft Excel®) gives a more detailed analysis of the radiance fits, and provides graphs of such fits. The spread sheet program does not run the NHA or NLLS algorithms; it requires information on the constants in OMT used to represent the radiance curve. Using the Microsoft Windows® environment we run both the FORTRAN program (in interactive mode), and the spread sheet program simultaneously to immediately analyze in detail the results of running NLLS-NHA algorithms and to view the graphs of the of the OMT fits as the adjustments are made to our methods.

3.2.2 FORTRAN Program. We chose the Levenberg-Marquardt method for the NLLS algorithm (Press, Flannery, Teukolsky and Vetterling, 1986). We took the basic algorithm from Press et al. and integrated it with the shell program, BFIT. BFIT breaks into six independent parts; (1) radiance data input, (2) initialize NHA fitting, (3) run NHA fitting, (4) initialize NLLS fitting, (5) run NLLS fitting, and (6) output solution parameters and fitted radiance profiles.

The input routine reads a data file which contains information on a particular TOVS scan. Each TOVS scan provides seven pairs of P-bar and Radiance values. When BFIT is run interactively, we choose one TOVS scan to test. In batch mode BFIT loops though all scans.

We integrated the original Non-Linear Hyperbolic fitting Algorithm to finish thoroughly analyzing that method and its usefulness. When running the NHA routine, we choose the number of constants to fit (e.g., a choice of four constants determines one constant term, one linear term, and one hyperbolic term) and then decide which channels to fit. The TOVS data has a total of seven channels.

Given a number of channels, the NHA fitting Algorithm provides a exact fit to those channels. The algorithm is numerically unstable owing to its character as an interpolation algorithm. Consequently, it provides very different solutions depending on which channels are chosen, and it cannot determine a solution for more than four channels of TOVS data. The NLLS NHA avoids these difficulties because it is not an interpolation algorithm.

BFIT runs the NLLS routine according to a script. The script determines which constants are to be varied and in what order. For example we choose a starting vector close to zero (presumably a bias-free choice) and we decide to release the constant and linear term only. The then algorithm fits the data with no hyperbolic terms. Then we release one hyperbolic term to see how it corrects the fit. The algorithm's performance also depends on a number of parameters such as the estimated errors in the data which weight different channels and the derivatives of the OMT constants which weight different terms in the curve. BFIT sets these parameters.

The NLLS is run according to the script, and it attempts to reduce the global χ^2 fit to the radiance data by varying the released constants. It provides what it determines as the best set of OMT constants for the fit.

BFIT reports the final OMT constants and provides a χ^2 per degree of freedom analysis of the OMT radiance curve fit to the original radiance data. This information is logged in a data file to maintain a record of each method's solution and performance.

3.2.3 Spread Sheet Program. The spread sheet program analyzes one scan in detail. All information on the scan is extracted from the data files used by the FORTRAN routines and presented in clear manner in one work sheet. The sheet contains the location and time of the scan, and lists in table form all information about each channel and the OMT curve match to that channel. The spread sheet program does several different error calculations in the tables.

We manually enter values for the OMT constant used to create the radiance curve. If we change the OMT constants on the work sheet, the spread sheet program immediately recalculates the OMT radiance curve and the error. A graphics sheet takes information from the work sheet and creates a graph of the radiance data points and the OMT curve. The graph is automatically updated when any changes are made on the work sheet. The spread sheet program quickly presents clear and detailed information on the OMT fit but does not provide information on how the fit was determined.

3.3 Reduction of TOVS Data to Atmospheric Temperature Profiles using OMT. We have readily available a set of 45 TOVS radiance scans, 15 from each of the three latitude zones. Each scan has corresponding radiosonde observations for comparison with the OMT temperature profile. These scans have been processed with the NLLS NHA software discussed in previous reports. (See, for example, Hohlfeld, Kilian, Drueding, and Ebersole 1988.)

Of the total of 45 TOVS scans processed, the complete set has yielded physically meaningful solutions involving a single hyperbolic term (with coefficients k_1 and L_1) and a linear term with coefficients a and b. Results of these runs are included in the Appendix. In each of the cases shown, values of k_1 were obtained, satisfying $-1 < k_1 \leq 0$, which corresponds to the new class of solutions discussed in the previous section.

Low latitude atmospheric temperature profiles exhibit a sharply defined tropopause feature, as evidenced by the radiosonde observations for the TOVS scans which we have studied. It is unrealistic to expect OMT fits based on only 4 terms to adequately represent such rapid variations of temperature with altitude. We plan to investigate whether this situation may be partially ameliorated by addition of a second hyperbolic term, or the addition of some other term to equation (8).

We have obtained meaningful fits to both long wavelength (667 cm^{-1}) and short wavelength (2250 cm^{-1}) TOVS data. However, as TOVS has only 5 short wavelength channels, we regard these bits as being less significant statistically than the long wavelength OMT fits.

Examples of NHA NLLS processing of TOVS data to OMT radiance and temperature profiles are given in Figures 4 through 7. For the TOVS data we have found that $m \approx 1$ is appropriate for representing TOVS weight functions and the corresponding representations of $E_m(x)$.

3.4. Discussion of the Results of TOVS Data Reduction. We have demonstrated that the NLLS NHA generates OMT fits on 100% of a set of 45 TOVS radiance scans from all latitude zones. Thus NLLS NHA is a robust algorithm suitable for processing TOVS data on a routine basis. Further advances in the construction of OMT fits, viewed as minimization problems in multidimensional parameter spaces, will allow more effective and efficient bias-free computation of OMT solutions.

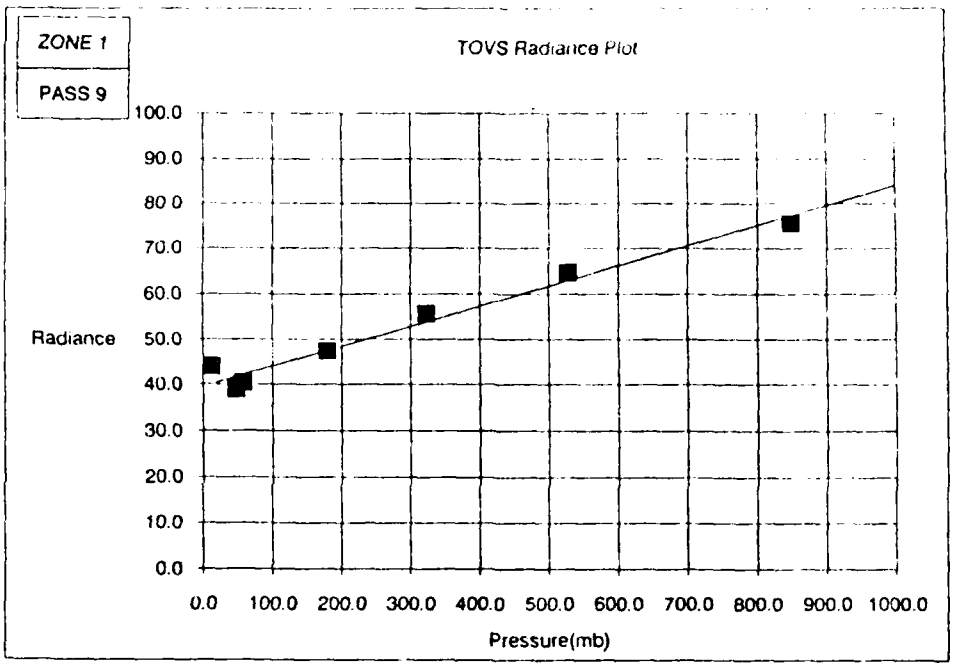

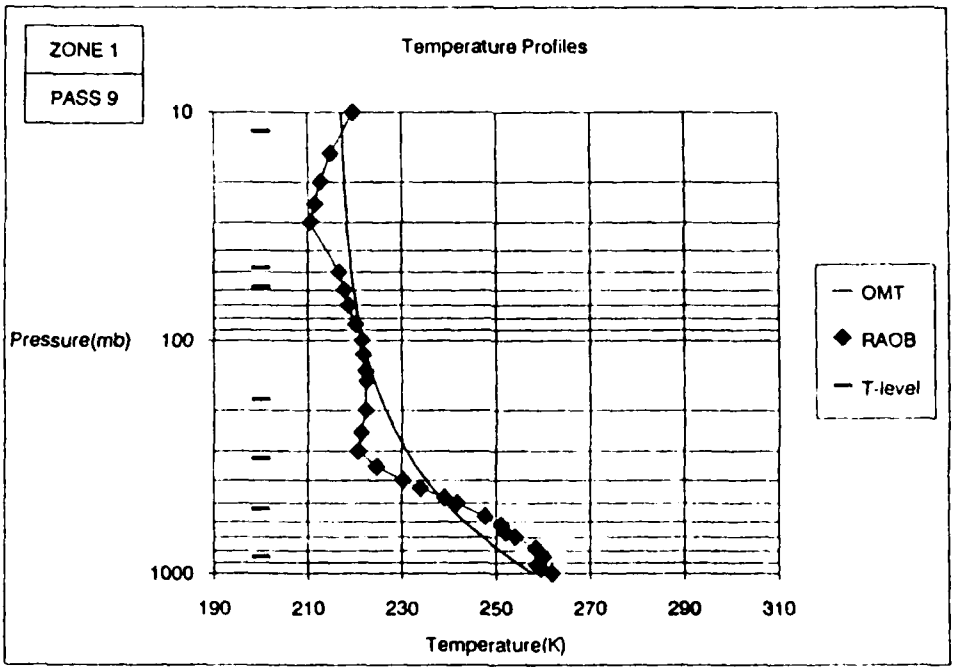

Figure 4: Optical Measure Theory radiance fit to TOVS data and temperature fit to RAOB data. This is a representative case of the fits achieved in Zone 1 by the Non-Linear Least Squares algorithm using OMT with four parameters for long wavelength data. The Non-linear least squares algorithm was given an initial vector with a = b = K_1 = 0 and L_1 = 10 and gave a solution with a = 20.23, b = 45.93, K_1 = 0.07889 and L_1 = 12.29 for Zone 1 Pass 9. This scan in Zone 1 was chosen because RAOB data was available up to 10 mb.

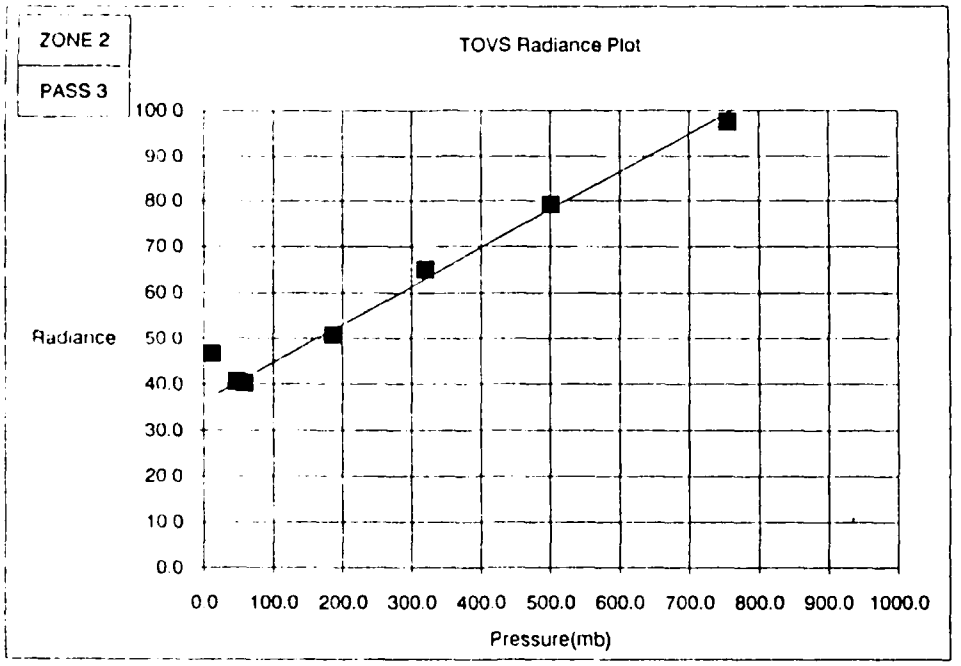

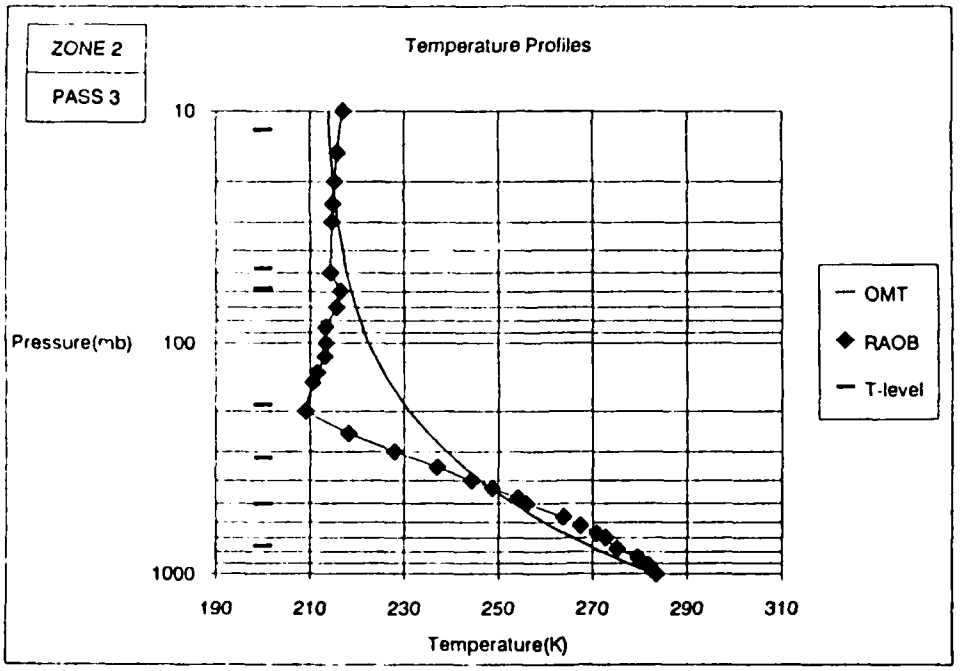

Figure 5: Optical Measure Theory radiance fit to TOVS data and temperature fit to RAOB data. This is a representative case of the fits achieved in Zone 2 by the Non-Linear Least Squares algorithm using OMT with four parameters for long wavelength data. The Non-linear least squares algorithm was given an initial vector with $a = b = K_1 = 0$ and $L_1 = 10$, and gave a solution with $a = 19.98$, $b = 85.54$, $K_1 = 0.1233$ and $L_1 = 16.29$ for Zone 2 Pass 3. This scan in Zone 2 was chosen because RAOB data were available up to 10 mb.

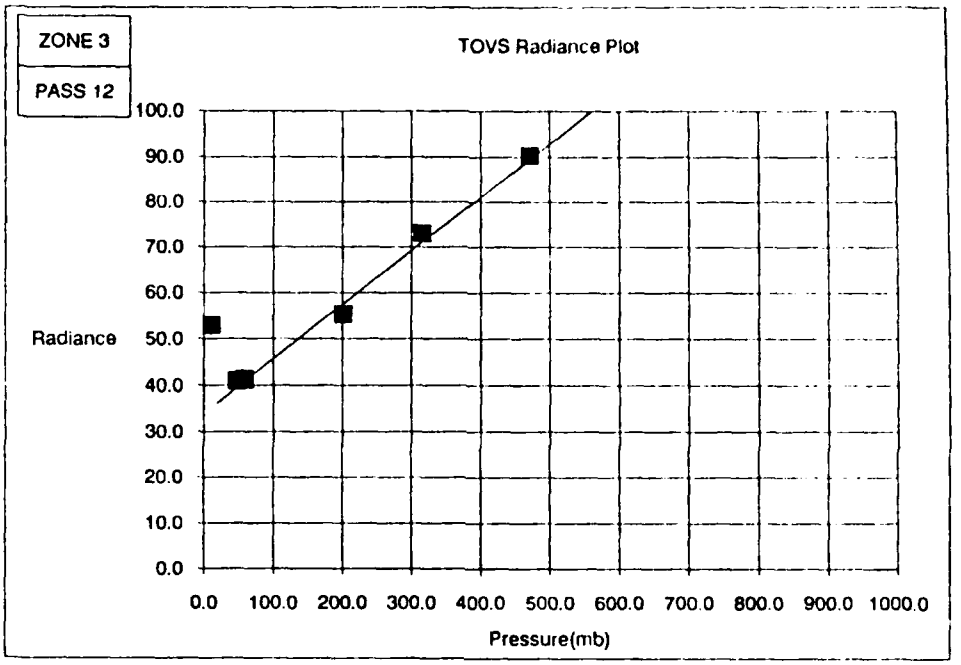

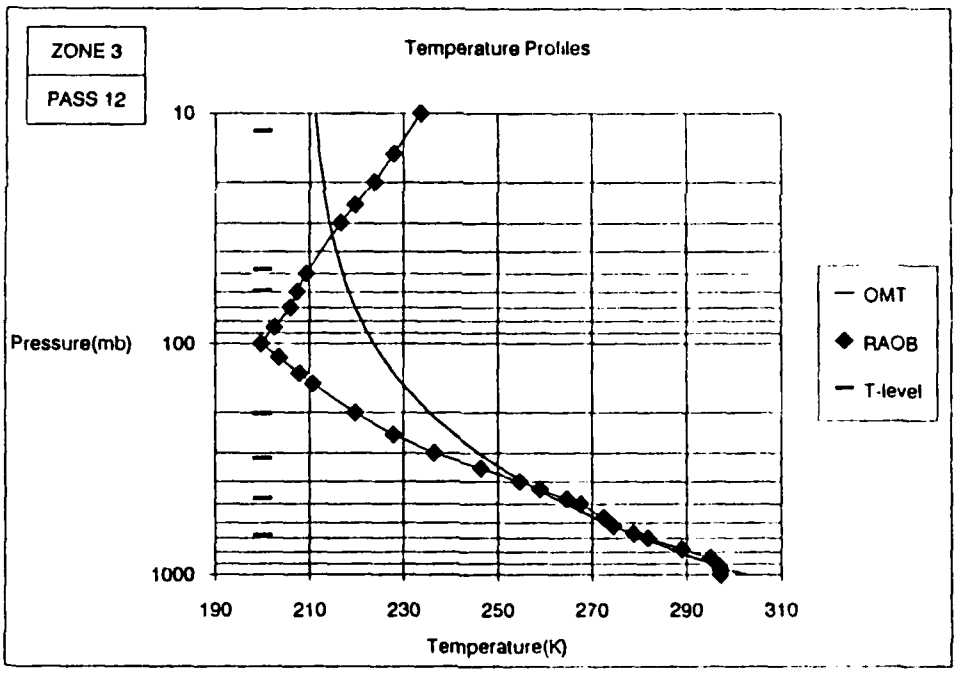

Figure 6: Optical Measure Theory radiance fit to TOVS data and temperature fit to RAOB data. This is a representative case of the fits achieved in Zone 3 by the Non-Linear Least Squares algorithm using OMT with four parameters for long wavelength data. The Non-linear least squares algorithm was given an initial vector with $a = b = K_1 = 0$ and $L_1 = 10$ and gave a solution with $a = 15.40$, $b = 117.7$, $K_1 = 0.008709$ and $L_1 = 18.49$ for Zone 3 Pass 12. This scan in Zone 3 was chosen because RAOB data were available up to 10 mb.

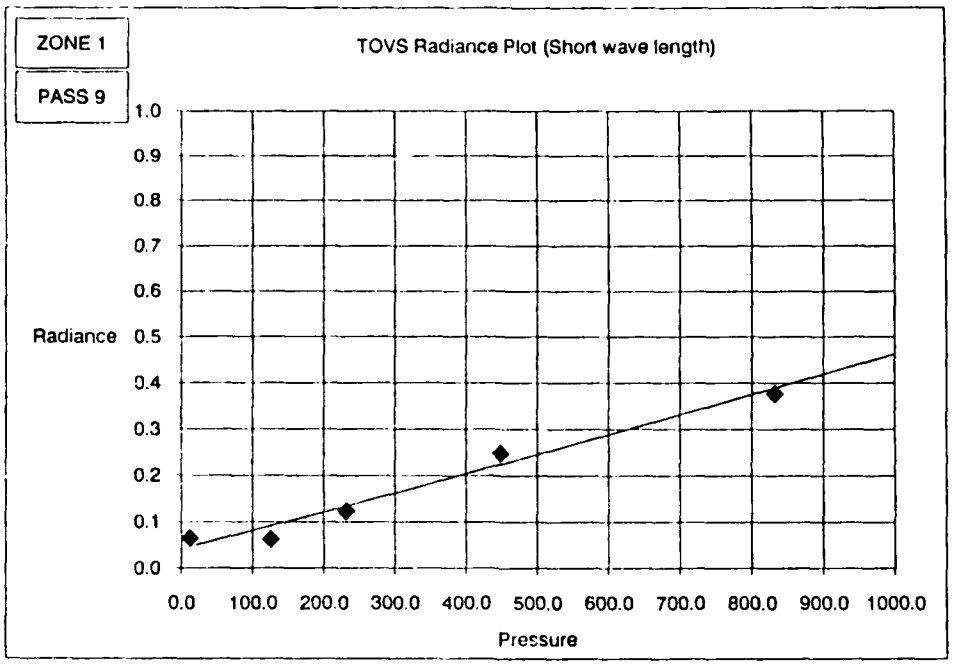

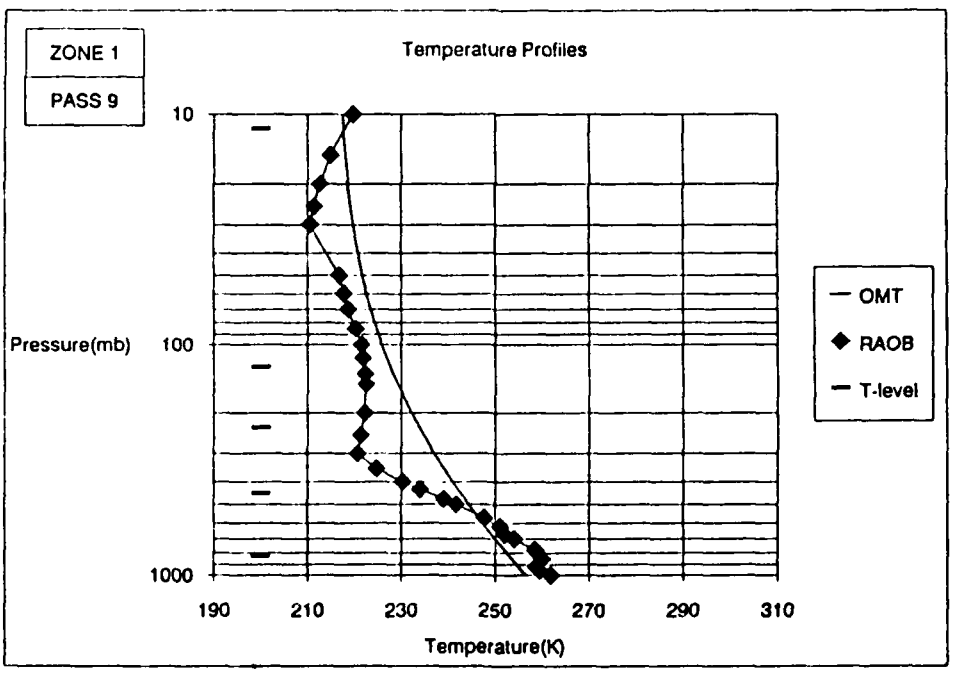

Figure 7: Optical Measure Theory radiance fit to TOVS data and temperature fit to RAOB data. This is a representative case of the fits achieved in Zone 1 by the Non-Linear Least Squares algorithm using OMT with four parameters for long wavelength data. The Non-linear least squares algorithm was given an initial vector with $a = b = K_1 = 0$ and $L_1 = 0.1$ and gave a solution with $a = -0.02927$, $b = 0.4591$, $K_1 = 1.1945$ and $L_1 = 0.07186$ for Zone 1 Pass 9. This scan in Zone 1 was chosen because RAOB data were available up to 10 mb.

It is highly interesting and scientifically significant that a meaningful OMT fit to the radiance data which yields a meteorological reasonable temperature profile can be constructed with just 4 parameters. First of all, this argues that the choice of functional form in equation (8) was an appropriate choice of the representation of radiance data. Secondly, it is highly suggestive that the actual information content of the TOVS radiance data is approximately equal to that which would be generated by 4 statistically independent channels (with relative errors characteristic of the TOVS radiometer). Such considerations are highly significant for the design of atmospheric sounders.

We note that the atmospheric temperature profiles obtained using the NLLS NHA exhibit a meteorological character and have a smooth form following the general trend of the radiosonde observations. The solutions we have obtained with $-1 < k_1 \leq 0$ are a significantly better match to the tropospheric temperatures than our previous set of solutions obtained for $k_1 > 0$. It cannot be expected that an OMT temperature profile constructed from a 4 parameter fit to the radiance data can match the detailed structure of the radiosonde observations. (In any event, the radiosonde observations available to us from NOAA may be as much as 3 degrees in latitude and longitude from the geographic location of the TOVS radiance observations.) However, it can be seen that we have captured the overall character of the actual atmospheric temperature profile in the OMT temperature profile. Further research will allow interpretation of the OMT fit parameters in more direct meteorological terms, such as tropopause temperature and pressure, and temperature lapse rates.

4. DIRECTIONS FOR FUTURE RESEARCH

The research undertaken during the Interim Research Period has demonstrated the utility of viewing the construction of OMT fits as minimization problems in a multidimensional parameter space, and has shown that these fits exhibit the meteorological characteristics desired. Furthermore, these algorithms are robust, working on our entire set of available TOVS radiance data. This represents an important milestone in the process of developing operational OMT capabilities. Further research tasks directed toward achieving that long-range objective can now be listed.

o Development of algorithms for global minimization on the radiance χ^2 surface utilizing nonlocal information on χ^2 geometry and allowing construction of nonlinear cost functions.

• Elucidation of the mathematical relationship between the parameters of the OMT fit and atmospheric structure parameters.

• Investigation of new data sets, so as to establish that the results we have obtained are not unique to the TOVS data set. Investigation of data sets with larger numbers of channels is particularly crucial.

• The theoretical formulation of OMT should be extended to include properly the effects of the ground, both in terms of its radiance and in terms of the truncation of atmospheric weight functions.

• Analysis of OMT algorithms should be undertaken from information theoretic principles to determine the information content of available radiance data sets and its bearing of the determination of the vertical temperature structure of the atmosphere.

In conjunction with the rest of our proposed Phase II research effort, considerable progress can be made leading to operational implementation of OMT algorithms.

5. CONCLUSIONS

We have demonstrated an implementation of Dr. King's Optical Measure Theory (OMT) based on mathematical concepts of χ^2 minimization on multidimensional parameter spaces. This approach is embodied in our NonLinear Least Squares Nonlinear Hyperbolic Algorithm (NLLS NHA). We have shown that the NLLS NHA is a robust algorithm for constructing OMT fits to TOVS radiance data, generating physically meaningful fits on 100% of a test sample of 45 scans. These fits were obtained both on long wavelength (700 cm^{-1}) and short wavelength (2250 cm^{-1}) TOVS data.

Acceptable fits to the TOVS radiance data were constructed using only 4 parameters in OMT. Such fits generate OMT temperature profiles with significant meteorological features. OMT temperature profiles are most appropriately employed in the remote determination of atmospheric structure parameters and for the determination of input parameters for numerical weather prediction codes, rather that replicating the small-scale temperature structures seen in radiosonde observations.

6. REFERENCES

Acton, F. S. (1970): **Numerical Methods that Work**, Harper and Row, New York

Chandrasekhar, S. (1960): **Radiative Transfer**, Dover, New York

Hohlfeld, R. G., J. C. Kilian, T. W. Drueding, and J. F. Ebersole (1988): "Novel Methodology for Application of Adaptive Systems Techniques for DMSP Remote Temperature Sensing", Creative Optics Report, COI-SR-26 to Air Force Geophysics Laboratory, Hanscom AFB, AFGL-TR-88-0323

Hopfield, J., and D. Tank (1985): Biol. Cybernetics, **52**, 141

Jeffrey, W. and R. Rosner (1986): "Optimization Algorithms: Simulated Annealing and Neural Network Processing", Astrophys. J., **310**, 473-481

King, J. I. F. (1985): "Theory and Application of Differential Inversion to Remote Temperature Sensing", in **Advances in Remote Temperature Sensing Methods**, A. Deepak, H. Fleming, and M. T. Chahine (Eds.), A. Deepak Publishing Co., Williamsburg, VA

King, J. I. F. (1989): "Optical Measure and the Non-Newtonian Calculus of Inverse Transfer Theory", private communication.

King, J. I. F., R. G. Hohlfeld, and J. C. Kilian (1989): "Application and Evaluation of a Differential Inversion Technique for Remote Temperature Sensing", Meteorology and Atmos. Phys., in press

Leon, S. J., and J. I. F. King (1988): "A Smart Algorithm for Nonlinear Interpolation and Noise Discrimination", presented at Int'l Workshop on Remote Sensing Retrieval Methods, Williamsburg, VA, 15-18 Dec. '87, Deepak Publ. Co., in press.

Marquardt, D. W. (1963): J. Soc. Ind. Appl. Math. 11, pp. 431-441.

Metropolis, N., A. Rosenbluth, M. Rosenbluth, A. Teller, and E. Teller (1953): J. Chem. Phys., 6, 1087

Press, W. H., B. P. Flannery, S. A. Teukolsky, and W. T. Vetterling (1986): **Numerical Recipes: The Art of Scientific Computing**, Cambridge University Press, Cambridge

APPENDIX

Results of Optical Measure Theory NLLS-NHA applied to TOVS long wavelength (700 cm-1) data:

ZONE 1

PASS	Parameters a	b	K1	L1	Radiance Chi Squared	Temperature Chi Squared
1	21.9897	52.4568	0.0712	18.8208	7.7253	9.6669
2	20.8109	50.8127	0.0754	20.7566	8.2237	12.5141
3	20.1024	36.1872	-0.0332	19.7633	10.9466	22.1108
4	20.6843	31.9178	0.0773	20.6341	8.0789	12.8196
5	20.2016	42.7945	0.0594	19.5847	8.2166	9.0614
6	24.1988	48.5561	0.0172	19.2390	4.5657	12.9135
7	20.0930	41.9455	-0.0228	19.3295	15.4449	25.6887
8	19.7153	42.3897	-0.0265	19.1709	11.9110	20.7550
9	20.2266	46.9303	0.0789	19.2882	8.5948	7.1561
10	21.0559	54.7609	0.0634	18.6387	8.7642	13.6989
11	21.0467	53.2192	0.0519	18.7438	8.3353	17.3833
12	20.6767	51.3538	-0.0291	18.8327	10.0275	15.5180
13	20.1530	41.7165	-0.0187	19.3757	16.4502	27.6259
14	20.7280	43.4540	0.0482	19.5211	5.8636	13.6721
15	20.8485	38.0441	-0.0966	19.7211	7.6981	13.1202

ZONE 2

PASS	Parameters a	b	K1	L1	Radiance Chi Squared	Temperature Chi Squared
1	20.0666	60.2591	-0.0134	18.4629	21.3097	14.0864
2	22.7040	46.1479	-0.5861	21.0458	26.5995	16.1779
3	19.9808	85.5354	0.1233	16.2895	24.6734	18.0511
4	23.6784	91.7270	0.0429	14.7175	47.5058	36.3018
5	22.5540	86.1593	0.0529	15.8039	39.4410	32.0148
6	25.4618	92.0344	0.0335	13.7685	49.9676	40.8259
7	24.4512	85.9867	0.0361	15.3968	44.2754	41.8214
8	23.4871	78.6828	0.0443	16.7173	35.0703	23.7176
9	13.9159	42.1279	-0.4681	28.6781	13.5568	10.4029
10	20.1966	61.0701	0.0021	18.5280	8.7407	15.1631
11	8.8821	33.2592	-0.4956	34.1463	10.5916	15.4403
12	17.8678	40.2948	-0.4735	24.2218	13.1907	7.9540
13	20.1134	76.6693	-0.2322	16.6688	23.4453	477.8820
14	24.7764	91.7628	0.0627	14.0435	42.4881	33.7657
15	18.6541	52.2492	-0.4316	23.9844	20.4876	12.4871

ZONE 3

PASS	Parameters a	b	K1	L1	Radiance Chi Squared	Temperature Chi Squared
1	17.5488	113.2630	0.0060	17.1666	72.7356	37.8103
2	22.5468	113.5100	0.0106	13.0646	64.9291	44.8249
3	21.6579	113.0420	0.1541	13.9088	67.5030	33.1921
4	20.9456	108.1440	-0.0603	14.3876	68.6499	60.4543
5	21.1345	110.9210	0.0556	14.1233	83.5579	50.9246
6	3.0187	79.4961	-0.4834	33.9501	80.9482	20.4364
7	17.8404	115.7700	-0.0049	16.4167	82.3276	43.6510
8	18.0460	114.8840	0.1531	17.0912	75.9672	40.5942
9	18.0460	114.8840	0.1531	17.0912	75.9672	43.3642
10	22.7688	118.1260	0.1193	12.3443	74.3194	55.5988
11	18.6673	112.6770	0.0669	16.7632	80.9567	47.7336
12	15.3976	117.6640	-0.0087	18.4916	80.4202	37.7834
13	22.3840	118.3220	0.1060	12.5496	66.9086	55.0465
14	20.1937	113.2730	0.2993	15.7100	63.9672	42.1414
15	22.1519	108.6000	-0.0683	13.7452	68.9993	73.7513

Results of Optical Measure Theory NLLS-NHA applied to TOVS short wavelength (2250 cm-1) data:

ZONE 1

PASS	Parameters a	b	K1	L1	Radiance Chi Squared	Temperature Chi Squared
1	-0.0817	0.5680	0.0135	0.1198	14.6169	22.7618
2	-0.0316	0.2224	-0.0609	0.0841	3.62269	15.7897
3	-0.0352	0.2807	-0.0266	0.0856	10.8188	31.4143
4	-0.0334	0.2322	-0.0352	0.0832	4.54404	15.6869
5	-0.0059	0.3429	0.0091	0.0571	9.80052	20.2758
6	-0.0722	0.5652	0.1163	0.1193	16.6156	22.4707
7	-0.0327	0.3440	-0.0110	0.0845	17.8615	40.0358
8	-0.0391	0.3646	-0.0261	0.0807	12.8574	32.0189
9	-0.0293	0.4591	1.1945	0.0719	9.6139	14.3352
10	-0.0806	0.5727	0.1443	0.1171	18.3589	25.0443
11	-0.0804	0.5674	0.1177	0.1150	17.2854	26.3545
12	-0.0307	0.5278	0.0062	0.0663	16.6639	28.3946
13	-0.0360	0.3494	-0.0022	0.0823	19.494	38.5053
14	-0.0965	0.3845	0.0136	0.1423	9.51026	24.4296
15	-0.2357	0.2529	-0.2399	0.2944	11.4666	26.0404

ZONE 2

PASS	Parameters a	b	K1	L1	Radiance Chi Squared	Temperature Chi Squared
1	-0.1773	0.4908	-0.2828	0.2238	29.3679	39.5405
2	-0.0366	1.1118	-45.3656	0.0745	7.26997	8.8E+16
3	0.0230	1.1199	-13.1211	0.0580	14.9585	51825.1
4	0.0983	1.1526	-9.8580	0.0367	39.7419	3397.62
5	-0.0186	1.2098	82776200	140509	61.1645	3703.7
6	-0.0939	1.2356	-2.8515	-0.0270	79.5673	122.164
7	0.1168	1.0552	-9.2818	0.0246	32.8007	1945.81
8	-0.1175	1.1452	3.4532	0.2170	82.7624	66.6798
9	-0.3895	0.4183	-0.5157	0.4347	29.9299	29.1776
10	-0.1438	0.4388	-0.4682	0.1942	24.3943	43.2193
11	-0.5422	0.2091	-0.5155	0.6007	30.3683	34.7671
12	-0.6453	0.0244	-0.5200	0.7203	32.2153	24.5781
13	0.0460	0.9901	-11.5321	0.0416	12.8681	12380.5
14	0.1019	1.2925	-3.1509	-0.0305	98.5834	129.156
15	-0.8287	0.2311	-0.4774	0.8978	56.7268	39.4245

ZONE 3

PASS	Parameters a	b	K1	L1	Radiance Chi Squared	Temperature Chi Squared
1	-4.4988	-0.1556	-0.2997	4.5656	178.66	120.195
2	0.0055	1.8417	-14.5069	0.1118	29.4934	647087
3	0.0093	1.7432	-14.3952	0.1058	24.6212	524511
4	0.0187	1.8322	-15.0639	0.1267	28.1215	2195220
5	0.0098	1.8336	-16.9123	0.1503	27.5544	76821500
6	0.0796	1.4105	-3.5775	-0.0234	151.232	112.93
7	-0.0459	1.9996	-20.8580	0.1666	26.67	2.73249E+11
8	-3.8965	0.1130	-0.2960	3.9548	184.67	126.902
9	-3.8965	0.1130	-0.2960	3.9548	184.67	137.046
10	0.0133	1.9180	-13.8175	0.1147	33.5552	262895
11	-0.0260	1.8946	-19.3872	0.1548	24.927	12825400000
12	-0.0752	2.1409	-22.3052	0.1747	27.8821	4.33052E+12
13	0.0119	1.9368	-14.7067	0.1238	30.9584	1080360
14	-4.6701	-0.1795	-0.2986	4.7380	173.639	131.566
15	0.0002	1.9937	-15.1188	0.1320	32.52	2970380